Computers and Concrete, *Vol. 25, No. 1* (*2020*) *29-36*
DOI: https://doi.org/10.12989/cac.2020.25.1.029

Modeling refractory concrete lining of fluid catalytic cracking units of oil refineries

Ana B.C.G. Silva[1a], Henrique C.C. Andrade[1b], Eduardo M.R. Fairbairn[*1], Jose C.F. Telles[1d], Fernando L.B. Ribeiro[1e], Romildo D. Toledo-Filho[1f] and Jorivaldo Medeiros[2g]

[1]Civil Engineering Department, Federal University of Rio de Janeiro, Centro de Tecnologia, Cidade Universitária, CEP 21945-970, Rio de Janeiro, RJ, Brazil
[2]Engineering Department, PETROBRAS, Centro, CEP 20231-030, Rio de Janeiro, RJ, Brazil

(*Received December 11, 2018, Revised November 24, 2019, Accepted January 4, 2020*)

Abstract. This work presents a numerical modeling procedure to simulate the refractory concrete lining in fluid catalytic cracking units of oil refineries. The model includes the simulation of the anchors that reinforce the contact between the refractory concrete and the steel casing. For this purpose, the constitutive relations of an interface finite element are set to values that represent the homogenized behavior of the anchored interface. The parameters of this constitutive relation can be obtained by experimental tests. The model includes also multi-surface plasticity, in order to represent the behavior of the refractory concrete lining. Since the complexity of real case applications leads to high computational costs, the models presented here were implemented in a high-performance parallelized finite element platform. A case study representing a riser similar to the ones used by the refinery industry demonstrates the potential of the model.

Keywords: numerical modeling; refractory concrete; concrete-steel interfaces

1. Introduction

The fluid catalytic cracking Unit (FCCU) is the primary producer of gasoline and olefins in the refinery. Although there are several designs of FCCU, they are generally composed by a reactor and a catalyst regenerator located in two separate vessels together with risers that connect these vessels to each other and to the rest of the refinery (see details in Chang *et al.* 2012). Since the temperature inside these vessels can reach from 520°C to 760°C, refractory concrete lining is used to drop these temperatures to a value that can be supported by carbon steel (about 400°C-530°C for short periods). The refractory concrete does not have a structural function. However, the thermo-mechanical effects on the lining may cause loss of adherence between concrete and steel, which makes part of the lining susceptible to fall off. Therefore, anchor systems are used to assure the adhesion of the refractory concrete on the steel casing. There are different types of anchorages. The most suitable choice depends on factors such as the thickness of the lining and the type of the concrete used.

Since the early 1950's, when refractory concretes, known as castables, made of calcium aluminate cements, were developed, a great effort have been made to improve their performance (Linck and Schlett 2014). In early applications, 18 months could be considered a very good period of operation between shutdowns. Nowadays periods of 6 to 7 years have already been reported for FCCU's without the need of significant maintenance. This was possible because several improvements have been made to the castables, concerning the material, the application, and the lining design (see, for example, Luz *et al*. 2015). In this context, the numerical modeling provides an important tool to analyze the behavior of steel/concrete structure under different conditions. Although numerical modeling of concrete has been studied with certain constancy over the years (Rodrigues *et al*. 2016), there are only a few references concerning refractory concretes. Buyukozturk and Tseng (1982) presented a study where refractory concrete was modeled by hexahedral elements while the steel vessel was modeled using membrane elements. The anchor was modeled with a one dimensional two node truss element. The refractory element had an orthotropic non-linear elastic constitutive relation. Both, truss and membrane elements, had a bilinear elastic-plastic strain hardening constitutive relation. Gasser *et al*. (2001) and Boisse *et al*. (2002) reported a FEM modeling approach in

∗Corresponding author, Professor
E-mail: eduardo@coc.ufrj.br
[a]D.Sc.
E-mail: eduardo@coc.ufrj.br
[b]M.Sc.
E-mail: henriqueconde@coc.ufrj.br
[c]Dr.Ing.
E-mail: eduardo@coc.ufrj.br
[d]Ph.D.
E-mail: telles@coc.ufrj.br
[e]D.Sc.
E-mail: fernando@coc.ufrj.br
[f]Ph.D.
E-mail: toledo@coc.ufrj.br
[g]M.Sc.
E-mail: jorivaldo@petrobras.com.br

http://www.techno-press.org/?journal=cac&subpage=8
ISSN: 1598-8198 (Print), 1598-818X (Online)

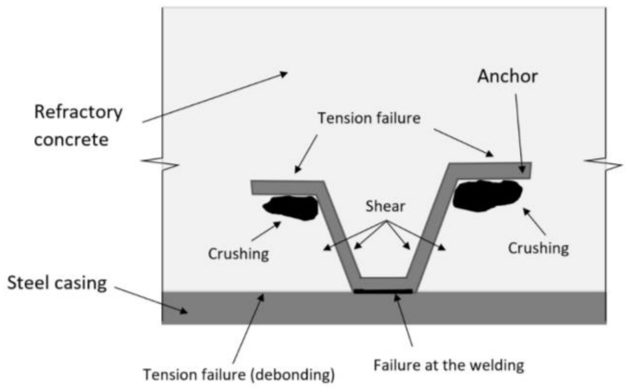

Fig. 1 Possible failures at the interfaces anchor-refractory and casing-refractory

two different scales. In a first step, a 3D local scale analysis considers the steel components and concrete as having different constitutive relations. The anchors and casing are considered as having an elastic-plastic behavior. The concrete is modeled by elasto-plasticity in compression and smeared cracking in tension. To model the vessel at the scale of the structure a two-layered shell element is used. The first layer represents the casing and has an elastic-orthotropic constitutive relation. The second layer has an elastic-damageable behavior. These two-layered shell elements have 16 parameters to be determined with the help of experimental tests and 3D modeling approaches using inverse analysis techniques. Many issues have to be dealt with when modeling refractory concretes. First of all, the properties of the materials are difficult to obtain due to the various temperature ranges continuously acting on the structures. Secondly, the presence of anchors at the steel-concrete interface may cause stress concentration and localized failure originated by the complex interaction between anchors and concrete. The steel-concrete interface has been studied in the literature mainly focusing on the interface between the reinforcing bars and the refractory lining (Angst *et al*. 2017). Certainly, it would be very difficult to implement a local model considering separately the anchors, the concrete and the steel casing. In the elastic domain, compatibility of displacements could be assumed. However, when the shear stresses in the anchor-refractory interface exceeds a certain threshold, the adhesion fails, and a bond slip model should be activated (see Fig. 1). Moreover, in regions where bonding is the mechanism of interaction, tension and compression failures may occur, becoming extremely complex to represent the local mechanical behavior. Even if it could be possible to implement a local model taking into account all these phenomena, the number of parameters involved would be excessively large. Yet, the determination of these parameters by experimental tests would probably consist of inverse analysis of macroscopic measurements. This means that the results of experimental tests, where only a few displacements are measured, would be used to determine a large set of parameters.

This paper presents the results of a research developed within the framework of a comprehensive joint project between PETROBRAS (The Brazilian national oil company) and the Federal University of Rio de Janeiro (UFRJ), that aims at improving the refractory lining performance used in FCCU's. In this way, a refractory material was developed with a percentage of steel fibers, increasing the fracture energy of the castable and thus enhancing its life in service. On the other hand, a 3D FEM model capable of simulating the thermo-mechanical behavior of the whole structure was developed. The interface steel/concrete is modeled by the interface element developed by De Borst and Schellekens (1993). The first novelty of this paper is the use of these interface elements to represent the anchorage, including a constitutive law representing the macroscopic behavior of the system steel/anchor/concrete. For this purpose, experimental tests were performed to better understand the behavior of this system. Therefore, the proposed numerical model uses only solid elements: a layer of interface elements between steel and concrete, and linear (tetrahedra) or trilinear (hexahedra) elements for steel and concrete. In the case study presented in this paper we use tetrahedral elements, due to its capacity of representing complex geometries and better computational performance. The anchor system formed by steel/anchor/concrete is discretized by patches of interface elements spanning an area with the same diameter as the samples used in the experimental tests.

Another contribution of this paper is the implementation of the multi-surface plasticity algorithm developed in Silva *et al*. (2015) to model the plastic behavior of the refractory fiber-reinforced concrete. Compressive failure is represented by a strain-hardening Druker-Pragger rule, while cracking is modeled by a strain-softening Rankine rule. The behavior of the steel casing is typically geometrically and elastic linear. This numerical model has been implemented in a high-performance 3D FEM code designed for parallel shared/distributed memory architectures, allowing analyses of complex structures. The parallelization techniques and high performance data structures and algorithms are the same as the ones presented in Ribeiro and Coutinho (2005), Ribeiro and Ferreira (2007) with some recent improvements on inter-process communication optimization for distributed/shared memory architectures, which are beyond the scope of the discussion here. Finally, a case study of an FCCU is presented, indicating that the proposed procedures may be employed for real-case engineering problems.

2. Mechanical behavior at the interface: experimental tests

In the present model, the interface behavior of the region affected by the anchors is considered by means of a homogenized constitutive law for the system steel/anchor/concrete. To determine this law, an experimental campaign was carried out. The mixture was prepared based on a dense refractory matrix with the addition of stainless steel fibers, with a volume fraction of 1.24%. In the last decades, the use of steel fibers as concrete reinforcement has been shown to be useful in several special applications (Mohod *et al*. 2012, Afroughsabet *et al*. 2016). This was also the case for refractory concrete where the use of fibers demonstrated

(a) Anchorage scheme (b) Test rig

Fig. 2 Sketch of the sample

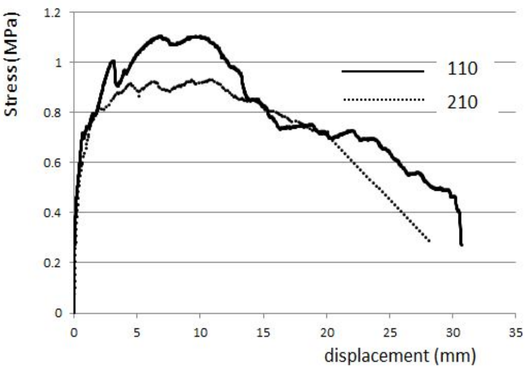

Fig. 3 Average response of the anchor system samples under tension tests

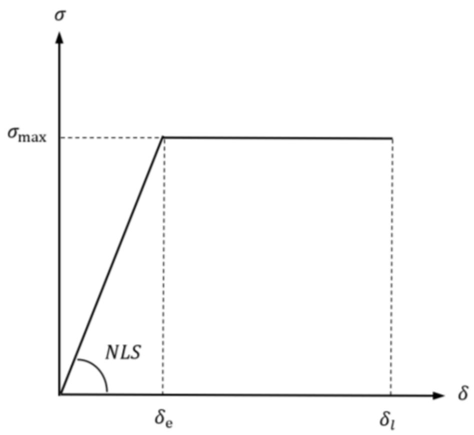

Fig. 4 Constitutive law for the anchor-concrete interface

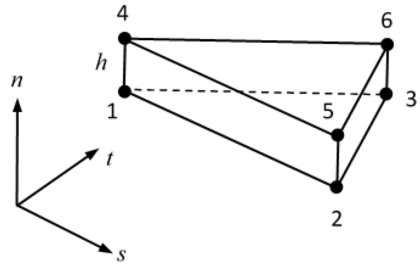

Fig. 5 Six-noded interface element

to increase the life cycle of the lining (Romano 2011). Two types of specimens were used: the first type consisted of steel disks molded together with the concrete cylinder and the second type had anchors welded to the steel disks and molded together with concrete cylinders. For each type of specimen, the samples were tested following specific temperature programs. In the first program the samples were first subjected to a temperature of 110°C and then the tests were carried out at room temperature. In the second program the sample was loaded at 210°C which is approximately the temperature at the interface between refractory and casing. Fig. 2 shows a sketch of the sample and a detailed test rig for high temperatures. A typical tensile test of the samples without anchors indicates that the refractory loses adhesion to the steel disk for very small loads that may be considered close to zero. Responses of tensile tests for specimens with anchors are given in Fig. 3, where the nominal stresses are computed in relation to the area of the cross section of the concrete sample. To obtain the constitutive relation in terms of stress versus displacement of the interface element, some simplifications have been made. First, it is considered that the interface opens with any positive displacement. For the opened interface, the stress-displacement law is considered as bilinear with a first region characterized by a constant named Normal Linear Stiffness (NLS). As the stresses reach a limit value ($\sigma_{\max}$, δ_e), they remain constant within the limiting prescribed displacement (δ_l), to guarantee a small displacement theory deformation (see Fig. 4).

3. Interface element

The formulation for the interface element presented here is based on De Borst and Schellekens (1993) and considers the six-noded interface element of Fig. 5. This element is an extension of a zero-thickness interface element found in Goodman *et al*. (1968).

For this element, each pair of nodes has initially the same geometrical coordinates, resulting in a zero-thickness element. The equations are obtained through the relative nodal displacements on the contact surfaces (Goodman *et* *al*. 1968). Each node has three degrees of freedom and the local displacement vector can be written as

$$\mathbf{u} = \{\mathbf{u}_{lower}, \mathbf{u}_{upper}\}^T \quad (1)$$

where

$$\mathbf{u}_{\boldsymbol{lower}} = \{n_1, s_1, t_1, n_2, s_2, t_2, n_3, s_3, t_3\}^T \quad (2)$$

$$\mathbf{u}_{\boldsymbol{upper}} = \{n_4, s_4, t_4, n_5, s_5, t_5, n_6, s_6, t_6\}^T \quad (3)$$

The relative displacements $\delta\mathbf{u}$ correspond to the difference between displacements of the upper and lower nodes

$$\delta\mathbf{u} = \mathbf{N}(\mathbf{u}_{lower} - \mathbf{u}_{upper})^T \quad (4)$$

being **N** the interpolation function matrix.

The stress vector at the interface element is defined by

$$\boldsymbol{\sigma} = \{\sigma_{nn}, \sigma_{ns}, \sigma_{st}\}^T \quad (5)$$

and can be obtained using the relation

$$\boldsymbol{\sigma} = \mathbf{D}\delta\mathbf{u} \quad (6)$$

To obtain the stresses at the interface element, the constitutive matrix **D** is

$$\mathbf{D} = \begin{bmatrix} d_{nn} & 0 & 0 \\ 0 & d_{ns} & 0 \\ 0 & 0 & d_{st} \end{bmatrix} \quad (7)$$

The terms d_{nn}, d_{ns} and d_{st} represent the normal and tangential stiffness. When in compression, these values are calculated as a function of the thickness *h*, the Young modulus *E* and the Poisson's ratio *ν* of the materials, through the relations

$$d_{nn} = E \cdot \frac{1}{h} \quad (8)$$

$$d_{ns} = d_{st} = \frac{E}{2(1+\nu)} \cdot \frac{1}{h} \quad (9)$$

where *h* is a very small number that represents the element thickness.

If the normal stress is a tension stress (σ_{nn}>0) the stiffness matrix is modified substituting the terms d_{nn}, d_{ns} and d_{st} for d_{nn}^*, d_{ns}^* and d_{st}^*. Two situations may occur:

(i) if the element does not contain an anchor, the coefficients of **D** are set to

$$d_{nn}^* = d_{ns}^* = d_{st}^* = 0 \quad (10)$$

(ii) if the element contains an anchor, the constitutive equation of Fig. 4 is activated and the following values are taken

$$d_{nn}^* = NLS \ \ if \ \ \sigma_{nn} < \sigma_{\max} \quad (11)$$

$$d_{nn}^* = 0 \ \ if \ \ \sigma_{nn} \geq \sigma_{\max} \quad (12)$$

$$d_{ns}^* = d_{st}^* = \frac{NLS}{2} \quad (13)$$

Considering the difficulty to obtain the parameters, we assume the interface behavior after the opening as being non-linearly elastic.

4. Multi-surface plasticity

The refractory lining is modeled by solid elements with multi-surface plasticity as described in detail in (Silva *et al*. 2015). Two different yield criteria are simultaneously applied: Rankine for (tension) and Drucker-Prager for compression, defined as

$$\text{Rankine:} \quad \sqrt{J_2}\left(\cos\theta - \frac{\sin\theta}{\sqrt{3}}\right) + \frac{I_1}{3} - f_t = 0 \quad (14)$$

$$\text{Drucker} - \text{Prager:} \quad \alpha\beta I_1 + \beta\sqrt{J_2} - f_c = 0 \quad (15)$$

where I_1 is the first invariant of the stress tensor, J_2 is the second invariant of the deviatoric tensor, θ is the Lode angle, f_t is the uniaxial tensile strength, and f_c is the uniaxial compressive strength. The Drucker-Pragger parameters are given by the following expressions

$$\alpha = \frac{k-1}{\sqrt{3}(2k-1)} \quad (16)$$

$$\beta = \frac{\sqrt{3}(2k-1)}{k} \quad (17)$$

$$k = \frac{f_{bc}}{f_c} \quad (18)$$

where f_{bc} represents the biaxial compressive stress.

5. FEM implementation

Real case applications of refractory concrete in FCCU's might have very complex three-dimensional geometries, always associated with non-linearity of the mechanical behavior. This leads to high computational costs, making unviable the simulation of real-world engineering problems. For this reason, the models presented here were implemented in a high-performance finite element platform. This platform was developed considering a parallel subdomain-by-subdomain approach and making use of compressed data structures, as described in Ribeiro and Coutinho (2005), Ribeiro and Ferreira (2007). This approach was originally designed for distributed memory architectures, with all communications being performed by MPI routines. However, it behaves very well in today's shared memory multicore computers, even when compared to multi-threaded OpenMP implementations (Batista *et al*. (2010)), as shown in Andrade *et al*. (2013).

There is a weak coupling between the thermal and mechanical models, in the sense that only the thermal strains affect the mechanical model. Due to changes of the physical parameters with temperature in both models, the coefficient matrices also change and the predictor/multi-corrector algorithm used for time dependent non-linear solutions had to be adapted to work on increments of the residual, rather than the residual itself. For the solution of the linear systems of both problems, the preconditioned conjugate gradients (PCG) method was employed. The original predictor/multi-corrector scheme, as well as the algorithms used to perform matrix-vector operations, are .

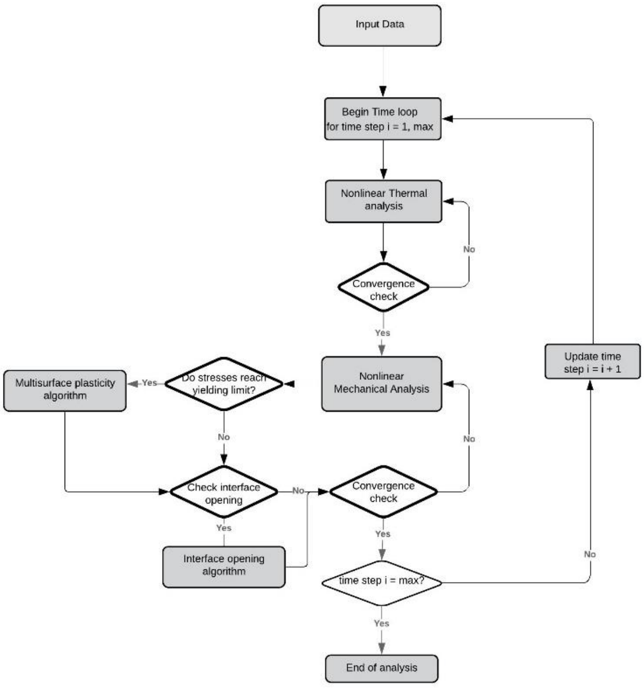

Fig. 6 Solution algorithm

Fig. 7 Refractory lining (left) and anchor system (right)

also described in detail in Ribeiro and Ferreira (2007). A flowchart illustrating the finite element solution algorithm is presented in Fig. 6.

6. Case study

The case study is the simulation of a refractory lining with an anchor system of the type shown in Fig. 7, where it can be seen an FCCU riser similar to the one studied in this paper, during maintenance.

6.1 Characteristics of the example

The main geometric characteristics and dimensions are presented in Fig. 8. This figure shows a cross section of the structure coinciding with the plane of symmetry. This cross section will be used to display mesh detail and results. The finite element mesh, composed of 1,829,125 4-noded tetrahedral elements and 363,894 nodes, is shown in Fig. 9. The anchor system pattern was obtained from the refractory concrete standards PETROBRAS N-1910 and N-1728.

According to the N-1910 standard, for a concrete thickness above 100 mm, the spacing between anchors must be between 200 mm and 400 mm. In this example, a

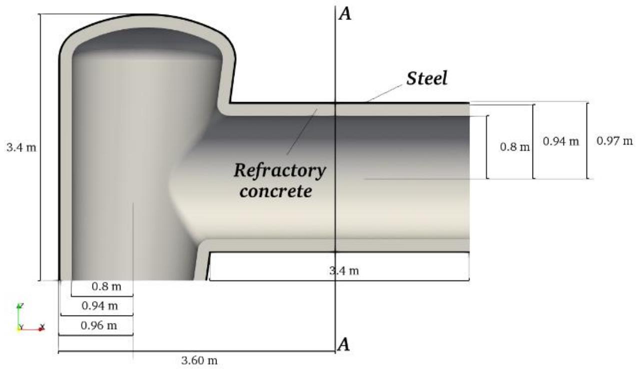

Fig. 8 Geometry of the top of the FCCU riser

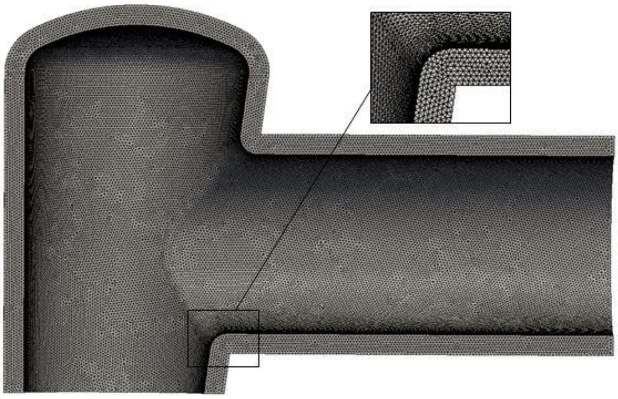

Fig. 9 FEM Mesh

spacing of 350 mm was considered. A view of the regions where the interface elements representing the anchors are placed is given in Fig. 10. This Figure represents the interface between steel and refractory concrete, with circles indicating the patches of anchor interface elements. At the internal surface a convective flux caused by a time dependent temperature of the fluid is prescribed. The convective heat exchange coefficient is taken as 141.96W/(m^2·ºC) (data provided by PETROBRAS). At external boundaries there is heat exchange with the environment, considering the environment temperature of 25ºC and a heat exchange coefficient of 56.78W/(m^2·ºC). For the present simulation, the internal fluid is linearly heated from an equilibrium temperature of 25ºC to 560ºC in one hour. It is maintained at 560ºC during 10 hours and then it linearly drops back to 25ºC in one hour. This process generates thermal gradients that produce tensile stresses necessary to induce the interface opening, activating the tensile behavior of the steel/concrete interface elements. There are no external forces, only constrained surfaces due to symmetry and constrained displacements in the z-direction. The properties were taken from Romano (2011), Franssen and Real (2015), ACI (1997).

The mechanical properties of the interface elements are NLS=1.61·109 N/m^3 and $\sigma_{\max}$=0.84 MPa. The mechanical properties of the refractory concrete are shown in Table 1. The temperature-dependent properties of the steel and the concrete are shown, respectively, in Tables 2 and 3, where α is the thermal expansion, k_t is the thermal conductivity and c_v is the volumetric heat capacity.

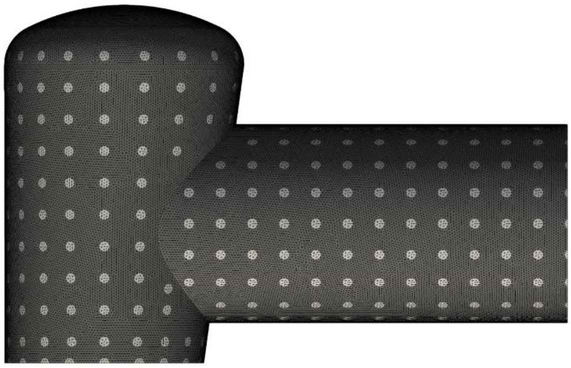

Fig. 10 Interface elements: the circles indicate the patches of anchor interface elements

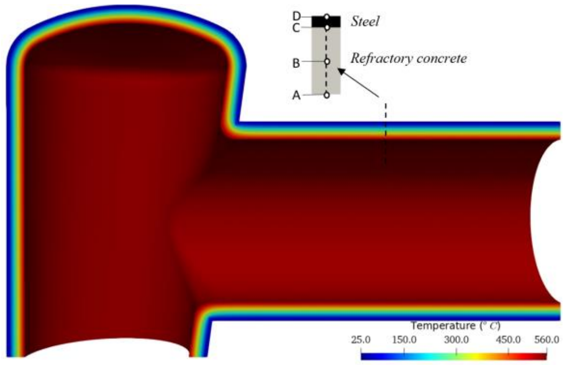

Fig. 11 Temperatures after 10 hours

Table 1 Mechanical properties of refractory concrete

$f_c(MPa)$	$f_{bc}(MPa)$	$f_t(MPa)$	$E(GPa)$	ν
60.6	72.7	3.9	28.3	0.2

Table 2 Mechanical and thermal properties of the steel

Temperature (°C)	20	200
$E(GPa)$	210	189
ν	0.3	0.3
α (10^{-6}/m^3·K)	11.0	12.0
k_t (W/m·K)	53.3	47.3
c_v (J/m^3·K)	$3.45\cdot10^6$	$4.16\cdot10^6$

Table 3 Thermal properties of refractory concrete

Temperature (°C)	20	200	400	600
α (10^{-6}/m^3·K)	5.0	5.0	5.0	5.0
k_t (W/m·K)	0.83	0.88	1.01	1.05
c_v (J/m^3·K)	$2.01\cdot10^6$	$2.12\cdot10^6$	$2.25\cdot10^6$	$2.37\cdot10^6$

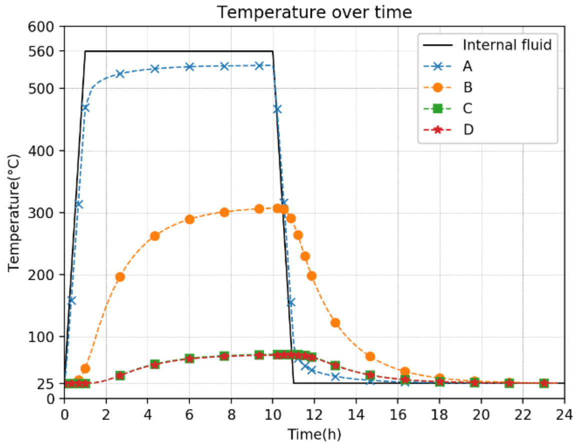

Fig. 12 Evolution of temperature in time

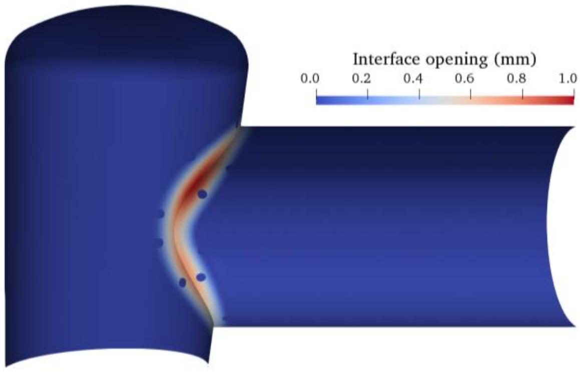

Fig. 13 Interface openings

6.2 Results

The temperatures of the analyzed structure are shown in Fig. 11, for a period of 10 hours. Fig. 12 shows the evolution in time of the temperature of the internal fluid: at the internal refractory surface (point A); at the center of the refractory lining (point B); at the interface concrete/steel (point C); and at the external surface (point D). These results show that, after 10 hours, when the changes in temperature are no longer significant, the refractory lining is efficient to ensure that the temperature of the steel will not exceed 400°C, which is the temperature supported by carbon steel. The regions where the refractory concrete separates from the steel are shown in Fig. 13. Maximum openings of the order of 1 mm can be noticed in the region where the two tubes are connected. The main effect that minimizes the separation of refractory and steel is obviously the action of the anchors. Fig. 14 and Fig. 15 indicate the regions of the riser that suffered plastification for the times of 1, 10, 11 and 24 hours. For the times of 1 and 10 hours, it can be seen that the external plastification (Rankine) of the refractory lining corresponds to a cracking tendency in this region. It is also noticed that there are some points in the internal surface that tends to crush (Drucker-Prager) by the effect of compressive strains. This tendency of cracking and crushing is coherent with the direction hot-cold of the thermal gradient from the internal to external surfaces. For the times of 11 and 24 hours, as the temperature drops in the interior of the riser, the temperature gradient inverts its direction inducing, as expected, cracking at the internal surface.

It should be stressed that the region of the connection between the horizontal and vertical parts of the structure concentrates stresses that are responsible for more intense plastification. The tendencies verified in the present simulation of cracking and crushing are the ones that can be verified in real cases as displayed in Fig. 16 for a riser similar to the present case study.

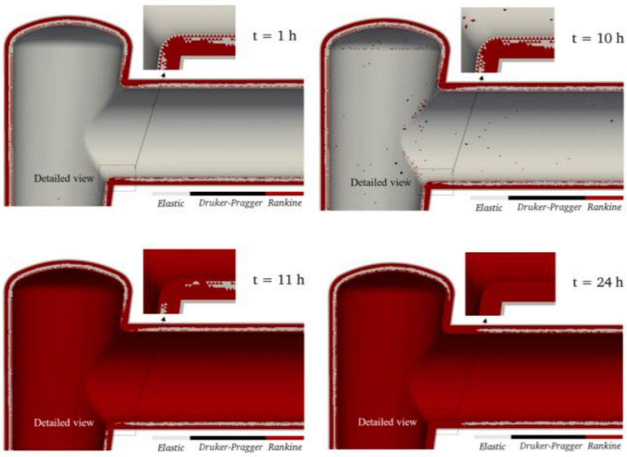

Fig. 14 Plastification for time=1 h, 10 h, 11 h and 24 h

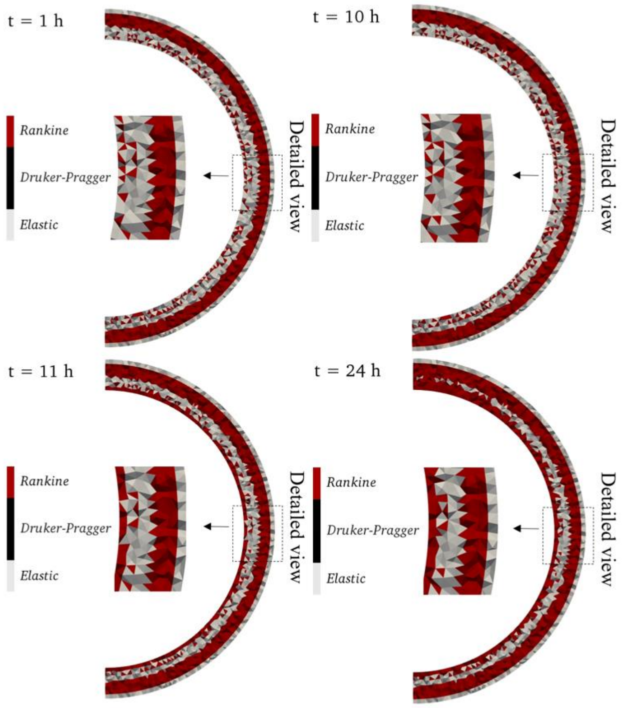

Fig. 15 Plastification at the cross-section AA for time=1 h, 10 h, 11 h and 24 h

7. Conclusions

This paper presented a computer model that is capable of simulating the very complex refractory lining problem of fluid catalytic cracking units, currently found in oil refineries. The typical nonlinear elastoplastic behavior of refractory fibers-reinforced concrete has been implemented using a multi-surface yield criterion discussed elsewhere. In addition, to simulate the anchored interface between the steel casing and the refractory lining, an interface element, with a special constitutive relation, was used. This relation introduces the macroscopic behavior of the interface region affected by the anchors into the computer simulation and can be determined by running experimental tests for its parameters. To illustrate the simulation capability, a case study, similar to a real situation, was thoroughly analyzed to demonstrate that the model can be used to accurately simulate the behavior of such fluid catalytic cracking units under high thermal gradients.

Fig. 16 Damage in a real structure similar to the riser analyzed in this paper

Acknowledgments

This study was financed in part by the Coordenação de Aperfeiçoamento de Pessoal de Nível Superior - Brasil (CAPES) - Finance Code 001. The authors also acknowledge the financial support of the Brazilian Scientific Agencies CNPq and FAPERJ, as well as PETROBRAS and the National Oil Agency ANP.

References

Afroughsabet, V., Biolzi, L. and Ozbakkaloglu, T. (2016), "High-performance fiber-reinforced concrete: a review", *J. Mater. Sci.*, **51**, 6517-6551. https://doi.org/10.1007/s10853-016-9917-4.

Andrade, H.C.C., Gonzaga e Silva, A.B.C. and Ribeiro, F.L.B. (2013), "Parallelization of the finite element method for distributed/shared memory architectures", *XXXIV CILAMCE - Ibero-Latin-American Congress on Computational Methods in Engineering*, Pirenpolis, XXXIVCILAMCE.

Angst, U.M., Geiker, M.R., Michel, A., Gehlen, C., Wong, H., Isgor, O.B. and Buenfeld, N. (2017), "The steel concrete interface", *Mater. Struct.*, **50**(43), 1-24. https://doi.org/10.1617/s11527-017-1010-1.

Batista, V.H.F., Ainsworth Jr., G.O. and Ribeiro, F.L.B. (2010), "Parallel structurally-symmetric sparse matrix-vector products on multi-core processors", arXiv:1003.0952, 17. https://doi.org/10.4203/ccp.101.22.

Boisse, P., Gasser, A. and Rousseau, J. (2002), "Computations of refractory lining structures under thermal loadings", *Adv. Eng. Softw.*, **33**, 487-496. https://doi.org/10.1016/S0965-9978(02)00064-9.

Buyukozturk, O. and Tseng, T.M. (1982), "Termo-mechanical behavior of refractory concrete linings", *J. Am. Ceram. Soc.*, **656**, 301-307. https://doi.org/10.1111/j.1151-2916.1982.tb10448.x.

Chang, A.F., Pashikanti, K. and Liu, Y.A. (2012), *Refinery Engineering: Integrated Process Modeling and Optimization*, Wiley VCH.

De Borst, R. (2008), "Numerical methods for the modelling of debonding in composites", Lecture Notes on Composite Materials-Current Topics and Achievements, Springer.

De Borst, R. and Schellekens, J.C. (1993), "On the numerical integration of interface elements", *Int. J. Numer. Meth. Eng.*, **36**(1), 43-46. https://doi.org/10.1002/nme.1620360104.

Franssen, J.M. and Real, P.V. (2015), "Fire design of steel structures", American Concrete Institute (ACI), ACI-547-R79, Refractory Concrete, Abstract of State-of-the-Art Report.

Gasser, A., Boisse, P., Rousseau, J. and Dutheillet, Y. (2001), "Thermomechanical behavior analysis and simulation of steel/refractory composite linings", *Compos. Sci. Technol.*, **61**, 2095-2100. https://doi.org/10.1016/S0266-3538(01)00155-5.

Goodman, R.E., Taylor, R.L. and Brekke, T.L. (1968), "A model for the mechanics of jointed rock", *JASCE J. Soil. Mech. Fdns. Div.*, **94**(3), 637-660.

Hermann, L.R. (1978), "Finite element analysis of contact problems", *J. Eng. Mech*., ASCE, **104**(5),1043-1057.

Kaliakin, V.N. and Li, J. (1995), "Insight into deficiencies associated with commonly used zero-thickness interface elements", *Comput. Geotech.*, **17**, 225-252. https://doi.org/10.1016/0266-352X(95)93870-O.

Linck, E. and Schlett, P.E. (2014), "60 years of petroleum & petrochemicals industry refractories history & opportunities for the future (You Snooze-You Lose!)", http://www.linckrefy.com/assets/60%20Years%20of%20Petroleum%20%20Petrochemical%20Refractories%20History.pdf.

Luz, A.P., Gomes, D.T. and Pandolfelli, V.C. (2015), "High-alumina phosphate-bonded refractory castables: $Al(OH)_3$ sources and their effects", *Ceram. Int.*, **41**, 9041-9050. https://doi.org/10.1016/j.ceramint.2015.03.276.

Mohod, M.V. (2012), "Performance of steel fiber reinforced concrete", *Int. J. Eng. Sci.*, **1**(12), 1-4.

Ribeiro, F.L.B. and Coutinho, A.L.G.A. (2005), "Comparison between element, edge and compressed storage schemes for iterative solutions in finite element analyses", *Int. J. Numer. Meth. Eng.*, **63**(4), 569-588. https://doi.org/10.1002/nme.1290.

Ribeiro, F.L.B. and Ferreira, I.A. (2007), "Parallel implementation of the finite element method using compressed data structures", *Comput. Mech.*, **41**, 31-48. https://doi.org/10.1007/s00466-007-0166-x.

Rodrigues, E.A., Manzoli, O.L., Bitencourt Jr., L.A.G. and Bittencourt, T.N. (2016), "2D mesoscale model for concrete based on the use of interface element with a high aspect ratio", *Int. J. Solid. Struct.*, **94-95**, 112-124. https://doi.org/10.1016/j.ijsolstr.2016.05.004.

Romano, G.Q. (2011), "Interface between steel and refractory concrete exposed to high temperatures: experimental analysis and computational modeling", Ph.D. Thesis, Federal University of Rio de Janeiro, RJ, Brazil. (in Portuguese)

Segurado, J. and Llorca, J. (2004), "A new three-dimensional interface finite element to simulate fracture in composites", *Int. J. Solid. Struct.*, **41**(11-12), 2977-2993. https://doi.org/10.1016/j.ijsolstr.2004.01.007.

Silva, A.B.C.G., Telles, J.C.F., Fairbairn, E.M.R., Ribeiro, F.L.B. (2015), "A general tangent operator applied to concrete using a multi-surface plasticity model", *Comput. Concrete*, **16**, 329-342. http://dx.doi.org/10.12989/cac.2015.16.2.329.

Wriggers, P. (2002), *Computational Contact Mechanics*, John Wiley & Sons.

CC